INTRAOPERATIVE SARCOMERE LENGTH MEASUREMENTS REVEAL DIFFERENTIAL DESIGN OF HUMAN WRIST EXTENSOR MUSCLES

RICHARD L. LIEBER[1,*], BJÖRN-OVE LJUNG[2] AND JAN FRIDÉN[3]

[1]*Departments of Orthopaedics and Bioengineering, Biomedical Sciences Graduate Group, University of California and Veterans Administration Medical Centers, San Diego, USA, [2]Department of Hand Surgery, Södersjukhuset, Stockholm, Sweden* and [3]*Department of Hand Surgery, Göteborg University, Göteborg, Sweden*

Summary

The design of the wrist extensor muscles was studied using a combination of intraoperative laser diffraction and biomechanical modelling of data obtained from human patients and previously published data. Intraoperatively, the change in sarcomere length per degree joint angle rotation (i.e. dSL/dω) was measured as the wrist was moved from neutral to full flexion in both the extensor carpi radialis brevis (ECRB) and extensor carpi radialis longus (ECRL) muscles. Sarcomere length change per degree rotation was approximately twice as great for the ECRB compared with the ECRL muscle (9.06±1.06 *versus* 4.69±1.20 nm degree^{-1}, mean ± S.E.M., *N*=7). Muscle fibre length and wrist extensor moment arms were obtained from published data and dSL/dω calculated. The experimental values for dSL/dω were extremely close to the calculated values. These data demonstrate that architectural differences between the ECRB and ECRL are accentuated by differences between their wrist extensor moment arms. This differential design may permit the extensor muscles, as a group, to generate high force over a wider range of velocities than would be possible with a single muscle or it may permit conservation of mass such that the two muscles together can generate approximately the same force and excursion as a single muscle but with approximately 30 % less mass.

Key words: wrist extensor muscles, sarcomere length, joint architecture, motor control, laser diffraction.

Introduction

Limb movement results from mechanical interactions between skeletal muscles, tendons and joints. The anatomy of these structures has been studied extensively at both the gross and microscopic levels (Butler *et al.* 1978; Ebashi *et al.* 1980; Gans, 1982; Huxley, 1974; Squire, 1981). Additionally, studies of muscle physiology, joint kinematics and tendon biomechanics have elucidated the functional properties of these anatomical structures. Recent efforts aimed at providing a more complete description of movement in humans and other animals have integrated the properties of the various components of the musculoskeletal system. For example, it was demonstrated that fish fast and slow skeletal muscles operate near the peak of their power–velocity relationships at near optimal sarcomere length (Rome *et al.* 1988, 1993; Rome and Sosnicki, 1991). During locomotion in cats, the medial gastrocnemius and soleus muscles are activated in such a manner as to exploit their metabolic and force-generating properties (Walmsley *et al.* 1978; Walmsley and Proske, 1981). Finally, frog skeletal muscles appear to be designed so as to maximize either power production during hopping (Lutz and Rome, 1994) or moment transfer in the bi-articular

musculature (Lieber and Boakes, 1988; Mai and Lieber, 1990). These studies suggest an impressive coordination among muscle, tendon and joint structural properties suited to their functional task(s).

Detailed anatomical studies of skeletal muscle demonstrated that the number of sarcomeres in series within a muscle (and thus, muscle fibre length) varies widely among muscles in both humans (Brand *et al.* 1981; Friederich and Brand, 1990; Lieber *et al.* 1992*b*; Van der Helm and Veenbaas, 1991; Wickiewicz *et al.* 1983) and other animals (Burkholder *et al.* 1994; Lieber and Blevins, 1989; Powell *et al.* 1984; Sacks and Roy, 1982; Zuurbier and Huijing, 1992). These studies have been interpreted to indicate that skeletal muscles can be anatomically specialized for force generation and/or excursion. For example, a muscle with relatively short fibres (and thus, few serial sarcomeres) arranged in a pennate fashion will produce higher force than a muscle of equal mass, but with longer fibres arranged in a more parallel manner. The longer-fibred muscle, however, will have a greater functional range over which force can be generated (Gans, 1982; Lieber, 1993). It is believed that, because muscles of varying designs are

placed throughout the musculoskeletal system, muscle capacity is matched to the particular functional tasks required.

Skeletal muscle sarcomere length represents an important anatomical variable that determines a muscle's relative force-generating capacity. It is thus important to describe the relationship between sarcomere length in a particular muscle and the joint on which it operates. If muscle moment arm is relatively large compared with the number of serial sarcomeres, sarcomere length change and thus force change will be large as the joint rotates, whereas the same muscle acting on a smaller moment arm will undergo a more modest force change during rotation. The sarcomere length change that occurs during joint rotation can be estimated from measured muscle and joint properties combined with an appropriate structural model. Alternatively, sarcomere length changes have been measured directly in fish (Lieber *et al.* 1992*c*) and humans (Fridén and Lieber, 1994; Lieber *et al.* 1994) and isolated muscle–joint preparations from frogs (Lieber and Boakes, 1988; Lieber and Brown, 1993) using optical laser diffraction. This method exploits the fact that the periodic striation pattern in skeletal muscle acts as a diffraction grating to incident laser light (Fig. 1). This type of measurement has the advantage that the sarcomere length change per degree of joint rotation is measured directly and is not calculated using assumptions regarding the relationship between muscle length and sarcomere length or the estimated joint kinematic changes during rotation.

Previous studies of sarcomere length change with joint angle in the frog hindlimb demonstrated a wide range of values from approximately 3 to 13 nm degree^{-1}, indicating different designs of muscle–joint complexes that are presumably tailored to frog locomotion (Lieber and Brown, 1993). We observed a similar diversity of design in the human wrist extensors in a single subject wherein the sarcomere length change was greater with joint rotation in the extensor carpi radialis brevis (ECRB) muscle than that in the extensor carpi radialis longus (ECRL) muscle (Lieber *et al.* 1994). However, these data were only from a single subject. In addition, since ECRB and ECRL are synergistic, their differential design could have functional importance in determining the range over which wrist extensor muscles could produce large forces and the magnitude of the forces themselves. To investigate the potential effects of the different designs of these synergists, sarcomere length changes in the human ECRB and ECRL during passive wrist rotation were measured.

Materials and methods

Intraoperative measuring device

The seven subjects included in this study were undergoing radial nerve release due to compression at the level of the supinator fascia. The ECRB and ECRL muscles were considered normal since the nerve compression occurred distal to the ECRB and ECRL motor branches. Patients ranged in age from 32 to 55 years and included five men and two women. All procedures performed were approved by the Committee on
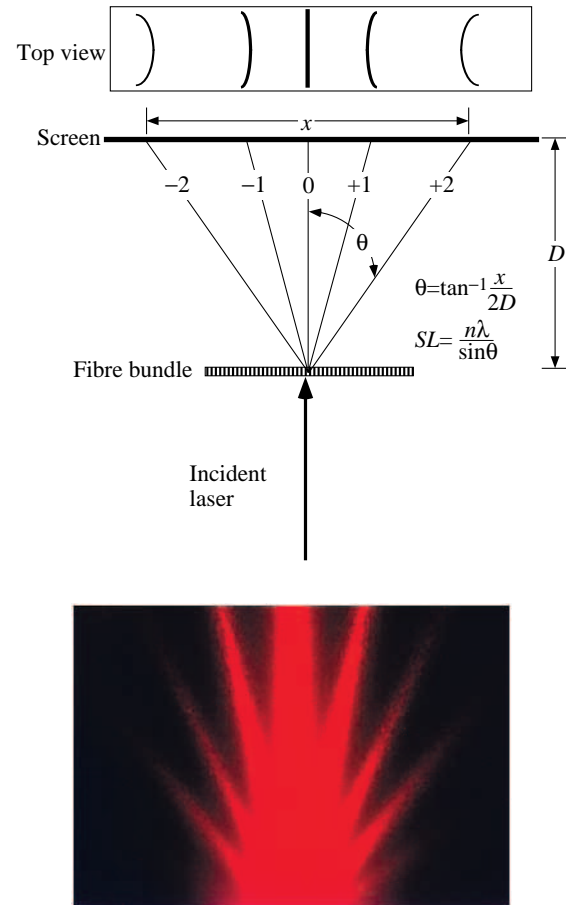

Fig. 1. Schematic diagram of the trigonometric arrangement for laser diffraction calibration and calculation. Sarcomere length is calculated using the equation, $n\lambda = SL\sin\theta$, where λ is the laser wavelength (0.632 μm), SL is sarcomere length, n is diffraction order, θ is diffraction angle, x is the spacing between second-order diffraction lines (−2 to +2), D is the distance from the exit face of the prism to the measuring screen. Inset: typical helium–neon laser diffraction pattern produced by human skeletal muscle.

the Use of Human Subjects at the University of Umeå, Sweden, and University of California, San Diego, USA.

The device used was a 7 mW helium–neon laser (Melles-Griot, model LHR-007, Irvine, CA, USA) onto which was mounted a custom-built device that permitted alignment between the laser beam and a small triangular prism (Melles-Griot, model 001PRA/001, Irvine, CA, USA). The laser beam was incident onto one of the short sides of the triangular prism, reflected off the aluminium-coated surface of the prism and exited 90 ° to the incident beam *via* the other prism face. Thus, the prism could be placed underneath a muscle bundle and transilluminated to produce a laser diffraction pattern (Lieber *et al.* 1994) (see Fig. 1, inset).

The diffractometer was calibrated using diffraction gratings of 2.50 μm and 3.33 μm spacings placed directly upon the prism. Diffraction order spacings from the second order were measured to the nearest 0.1 mm using dial calipers which corresponded to a sarcomere-length resolution of

approximately 0.05 μm. Repeated measurement of the same diffraction order spacing by different observers resulted in an average calibration of the 3.33 μm grating as 3.38±0.13 μm (mean ± S.D., *N*=25).

Experimental protocol

Immediately after administration of regional anaesthesia, the distal ECRB and ECRL were exposed using a dorsoradial incision approximately 10 cm proximal to the radiocarpal joint. The overlying fascia was divided, exposing the underlying muscle fibres. A small fibre bundle was isolated near the insertion site using delicate blunt dissection in a natural intramuscular fascial plane, taking care not to overstretch muscle fibres. Since both muscles have a characteristic appearance in this distal region, care was taken to isolate muscle fibres from the same region in all patients studied.

The illuminating prism was inserted beneath the isolated fibre bundle and approximated into the normal plane of the muscle. Sarcomere length was measured with the bundle in the *in vivo* position, maintaining precautions against elevation of the fibre bundle (which would cause artefactually long sarcomere lengths). Because fibre bundles were isolated only from the distal 2 cm of each muscle, we cannot determine the extent to which these data are representative of the entire muscle. In anatomical studies of similar formalin-fixed human muscles (Lieber *et al.* 1990), sarcomere length variations along the entire muscle fibre length rarely exceed 0.3 μm.

Dial calipers were used to measure the spacing (*x*) between the second-order diffraction lines. This distance was converted to diffraction angle (θ), assuming that the zeroth diffraction order bisected the second-order lines, using the equation $\theta=\tan^{-1}(x/2D)$, where *D* is the distance from the exit face of the prism to the measuring screen (Fig. 1). The value of *D* was calculated previously using diffraction gratings of 2.50 μm and 3.33 μm spacings. (Any diffraction order spacing can be used in this equation. The second order was chosen since it has a convenient spacing and is intense enough to be easily discernible.) Sarcomere length was then calculated using the equation $n\lambda=SL\sin\theta$, where λ is the laser wavelength (0.632 μm), *SL* is sarcomere length and *n* is diffraction order.

ECRB and ECRL sarcomere lengths were measured in each subject with the elbow 20 ° from full extension and the wrist placed in each of three positions: full flexion (average radiocarpal angle of approximately 40 ° of flexion), neutral (average of approximately 10 ° of extension) and full extension (average of approximately 50 ° of extension). The angular value corresponding to each position was measured with a goniometer. When the wrist was fully extended, in two subjects, the muscle became slack, precluding accurate sarcomere length estimates. Thus, values used to quantify the slope of the sarcomere length change/joint angle relationship (i.e. d*SL*/dω), where ω is wrist joint angle, were obtained from the slope of the line connecting the data points obtained with the wrist in the flexed and neutral positions.
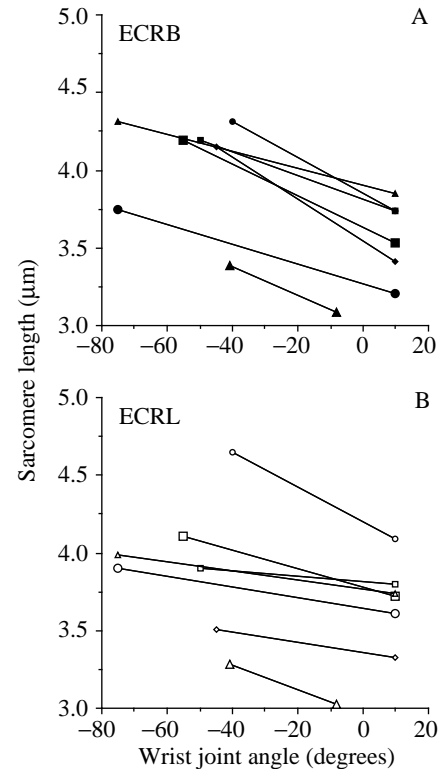

Fig. 2. Raw sarcomere length data obtained for flexed (negative joint angles) and neutral (positive joint angles) wrist joint angles for seven human subjects. Each symbol refers to a single subject. Filled symbols represent ECRB muscles (A), open symbols represent ECRL muscles (B).

Results

Raw intraoperative data

Moderate variability between subjects was found for absolute sarcomere lengths (Fig. 2). Some of this variability probably reflects true differences between subjects while some probably represents variations in patient positioning that could not be controlled. For all seven subjects studied (corresponding to the different symbols in Fig. 2), the slope of the sarcomere length–joint angle relationship was greater for the ECRB than for the ECRL (Table 1). These sarcomere lengths are significantly longer than those found in frog or fish muscle, owing to the longer actin filaments contained in human muscle (Walker and Schrodt, 1973). Quantitative electron microscopy of human ECRB muscle tissue previously revealed actin filament lengths within half of the I-band of 1.30±0.027 μm (mean ± S.E.M., *N*=24) while myosin filaments were 1.66±0.027 μm long, yielding an optimal sarcomere length of 2.60–2.80 μm and a maximum sarcomere length for active force generation of 4.26 μm (Lieber *et al.* 1994) compared with an optimal sarcomere length of 2.20 μm and a maximum sarcomere length for active force generation of 3.65 μm in frog and fish muscle (Gordon *et al.* 1966; Sosnicki *et al.* 1991).

Average slope of ECRB and ECRL relationships

To calculate the slope of the sarcomere length change per

Table 1. *Sarcomere length changes in wrist extensor muscles*

	Sarcomere length change per degree joint angle rotation		
Subject	ECRB muscle (nm degree^{-1})	ECRL muscle (nm degree^{-1})	ECRB/ECRL ratio
L.M.	−11.4	−11.2	1.02
S.S.	−10.2	−6.00	1.69
I.O.	−7.50	−1.67	4.49
R.H.	−5.41	−2.94	1.84
A.L.	−13.45	−3.27	4.11
R.P.	−6.35	−3.41	1.86
I.M.	−9.09	−4.31	2.11
Mean ± s.e.m.	−9.06±1.06	−4.69±1.20	2.45±0.49

Values are given as nm degree^{-1} wrist extension.

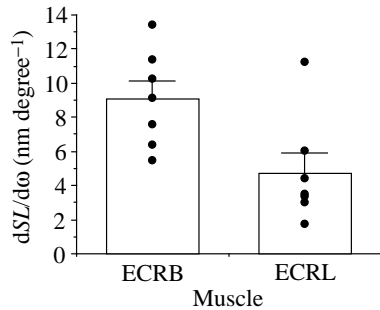ECRB, extensor carpi radialis brevis; ECRL, extensor carpi radialis longus.

Fig. 3. Slope (dSL/dω) of the sarcomere length–joint angle relationship for the ECRB and ECRL muscles. Values are calculated as sarcomere length change per degree joint extension and are thus negative numbers since sarcomeres shorten with wrist extension. They are plotted as positive values for convenience.

degree wrist rotation relationship, dSL/dω, we restricted our consideration to data points obtained between full wrist flexion and the neutral position. This was because, in two cases, it was noted that the muscle became slack during full extension and, since the muscles were not activated, we did not believe that the values obtained with the wrist extended represented the true physiological condition. A relatively large degree of variability in dSL/dω was observed between subjects for both the ECRB and ECRL (Fig. 3). For example, ECRB dSL/dω ranged from −5.4 to −13.5 nm degree^{-1} while values for the ECRL ranged from −1.7 to −11.2 nm degree^{-1}. Across all subjects, average dSL/dω for the ECRB was −9.06 nm degree^{-1} while that of the ECRL was approximately half this value, 4.69 nm degree^{-1} (Table 1). We calculated the ratio of dSL/dω values between the ECRB and ECRL for each subject and averaged these values across subjects. This mean dSL/dω ratio for the intraoperative sarcomere length data was 2.45 (Table 1).

Discussion

The purpose of this investigation was to compare the

Table 2. *Anatomical data used to predict sarcomere length changes*

Parameter	ECRB value	ECRL value
Fibre length (mm)	48	76
Optimal sarcomere length (μm)	2.8	2.8
Number of serial sarcomeres	17 143	27 143
Integrated wrist moment arm (mm)	11.37	6.94

Muscle architectural data are from Lieber et al. (1990) and wrist moment arm values are from Loren et al. (1996).

sarcomere length changes of the ECRB and ECRL muscles during wrist joint rotation. Our main finding was that these muscles, while synergistic in terms of their location and pattern of activation (Bäckdahl and Carlsöö, 1961; McFarland *et al.* 1962; Riek and Bawa, 1992), have quite different anatomical designs that are predicted to produce different functional properties of the muscle–tendon–joint torque-generating system.

To predict the expected ratio between dSL/dω values for the two muscles, muscle lengths and the number of serial sarcomeres were obtained from upper extremity architecture data (Lieber *et al.* 1990) whereas wrist extensor moment arms were obtained from published kinematic data (Loren *et al.* 1996) (Table 2). Sarcomere length change during wrist extension was thus modelled by integrating the moment arm equation over the range from approximately 40 ° of flexion to approximately 10 ° of extension (the average flexed and neutral positions respectively) for the ECRB (Table 2):

$$r_{\text{ECRB}} = \int_{\omega=-0.5}^{\omega=0.25} 16 + 8.95\omega + 2.84\omega^2 - 11.0\omega^3 - 12.9\omega^4, \quad (1)$$

and for the ECRL:

$$r_{\text{ECRL}} = \int_{\omega=-0.5}^{\omega=0.25} 10.5 + 9.99\omega, \quad (2)$$

where wrist joint angle (ω) is in radians and negative angles refer to wrist flexion. Given the relationship between muscle excursion (s), moment arm [$r(\omega)$] and angular rotation (ω) of ds=rdω, the ratio of sarcomere length changes with wrist extension for the two muscles is given by the expression:

$$\frac{\text{d}SL_{\text{ECRB}}}{\text{d}SL_{\text{ECRL}}} = \frac{r_{\text{ECRB}} \times N_{\text{ECRL}}}{r_{\text{ECRL}} \times N_{\text{ECRB}}}, \quad (3)$$

where dSL is the change of sarcomere length with joint rotation (i.e. dSL/dω) and N is the number of serial sarcomeres. The integrated moment arms for ECRB and ECRL were 11.37 and 6.94, respectively, while the numbers of serial sarcomeres were 17 143 and 27 143, respectively (Table 2). Inserting these values into equation 3 yields a sarcomere length change ratio of 2.57, which is close to the experimentally measured value of 2.45 (Table 1). This close agreement not only supports the modelling approach but also permits us to use this mechanical model to predict the joint moment of the wrist extensors with confidence.
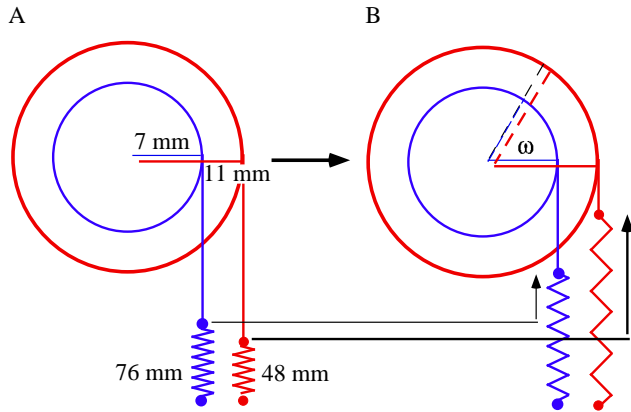
Fig. 4. Schematic diagram of the interrelationship between fibre length and moment arm for the ECRB and ECRL torque motors. The diagram represents the wrist joint in the neutral (A) *versus* extended (B) position. The wrist joint is represented as two concentric pulleys (circles) of differing diameters to approximate the two different moment arms. The ECRB (red lines) with its shorter fibres (48 mm) and longer moment arm changes sarcomere length approximately 2.5 times as much as the ECRL (blue lines) with its longer fibres (76 mm) and smaller moment arm (see Table 2). ω, wrist joint angle.
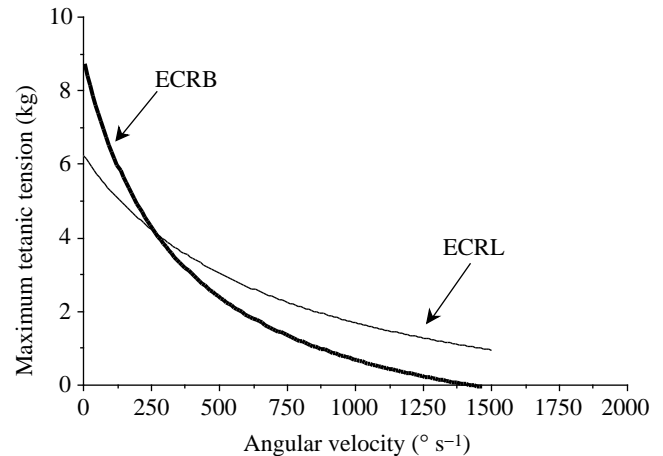

Fig. 5. (A) Calculated force–velocity relationships for the ECRB and ECRL muscles based on muscle architecture and wrist joint moment arms. The two curves cross at an angular velocity of approximately $240°\,s^{-1}$ which, on the basis of the muscle moment arms, corresponds to a muscle velocity of approximately $80\,mm\,s^{-1}$.

The general factors that affect the torque-generating capacity of a muscle–tendon–joint unit (described here as a 'torque motor') were described in experimental studies leading to a theoretical model of the wrist flexors and extensors (Lieber *et al.* 1990; Loren and Lieber, 1995; Loren *et al.* 1996). The thesis is that muscles, tendons and joints interact to produce a torque motor with well-defined properties and that the muscles, tendons and joints have properties that are complementary to one another. In the context of the current study, the major factor determining the properties of the torque motor is the ratio between the moment arm and the number of sarcomeres in series within the muscle. Using ordinary muscle architectural terminology, this would be expressed as the moment arm:fibre length ratio (Zajac, 1992). From a design point of view, a high moment arm:fibre length ratio results in a torque motor in which large fibre length changes produce large force changes during joint rotation and, thus, this motor would vary its torque output to a great extent as the joint rotated. This approximates the design of the ECRB torque motor for wrist extension motions, based on its relatively short fibres and large moment arm (Fig. 4). In contrast, the significantly longer fibres and smaller moment arm of the ECRL result in a torque motor with different functional properties. The ECRL-based motor retains a more constant torque output with joint rotation since, for a given amount of joint rotation, sarcomere length changes less (Fig. 4). In radial deviation, the situation is quite different. In this case, the increased ECRL radial deviation moment arm compared with that of the ECRB almost exactly matches the fibre length ratios (Loren *et al.* 1996). Thus, for radial deviation movements, the sarcomere length change per radial deviation angle for both muscles is probably nearly equivalent. The fact that the ECRL has a substantial moment arm at the elbow while the ECRB

has almost none does not seem to provide insight into its long-fibred design. The functional effect of such a design would be to maintain sarcomere length relatively constant in the ECRL with simultaneous wrist flexion and elbow extension, while not affecting ECRB function.

Dynamically, the situation may be more complex since the architectural design that favours isometric force production may be disadvantageous in the dynamic situation (Gans and De Vries, 1987). For example, the ECRB has a higher predicted maximum tetanic tension than the ECRL (8.75 kg *versus* 6.25 kg; Lieber *et al.* 1990) because of its greater number of shorter muscle fibres. Yet, since these fibres are shorter, for a given angular velocity (assuming similar fibre-type proportions), force relative to maximum isometric tension decreases to a greater extent in the ECRB (Fig. 5). Using the architectural properties of the two muscles (Lieber *et al.* 1990), along with nominal values for the maximum contraction velocity (V_{max}) of mammalian muscle (Close, 1972), the force–velocity relationship for each muscle can be determined. The exact values for V_{max} and the force–velocity curvature are not important in making this comparison as long as the ECRB and ECRL fibre-type distributions are not dramatically different from one another. The contraction velocity at which the ECRL becomes stronger is approximately $80\,mm\,s^{-1}$ which, on the basis of the two muscle moment arms, corresponds to an angular velocity of approximately $240°\,s^{-1}$ (Fig. 5). This results in a design in which the ECRB is stronger isometrically, but the ECRL becomes the stronger muscle as angular velocity increases.

This differential muscle strength that is velocity-dependent may provide insight into the diversity of design between muscles. The ECRB and ECRL muscles as a synergistic group have a maximum tetanic tension of 25.6 kg and a V_{max} of approximately $2800°\,s^{-1}$. In order for a single muscle to generate that much force while maintaining such a high V_{max},

the fibre length would have to be 76 mm (as for the ECRL to maintain the same V_{max}) and the cross-sectional area would have to be approximately $4.2 \, cm^2$ (the sum of the two muscles' physiological cross-sectional areas to maintain the same maximum force). Using the simple equation for muscle physiological cross-sectional area (Sacks and Roy, 1982), this single muscle would weigh 33.7 g, which is over 30 % greater than the sum of the two muscle masses (Lieber *et al.* 1990). Having two muscles as synergists thus accomplishes the same task at the velocity extremes but with a lower mass.

Limitations of this study

This study has several limitations. First, sarcomere lengths were measured only at three joint angles. Obtaining more data throughout the range of joint motion would influence the shape of the curve, but would not change the relative differences between these muscles. Second, the neural activation patterns involved in normal movement were not considered. Effectively, the muscle was modelled as a large sarcomere. This neglects the elegant arrangement of motor units within the muscle that results in the wide range of force generation that is possible (Henneman *et al.* 1965) and the sarcomere length dispersion that exists in whole skeletal muscles. In fact, in view of the intriguing data of Petit *et al.* (1990) that different unit types have different stiffness values, it may be that different motor unit populations actually have different length–tension relationships. This potentially sophisticated coordination between motor units and muscle fibres deserves further study.

The current study should thus be viewed as a description of the 'anatomically possible' joint moments developed by the ECRB and ECRL but not necessarily those that are actually used. Finally, because conclusions from this study are based on passive sarcomere length, the effects of series muscle and tendon compliance are neglected. However, we have previously explicitly measured human wrist tendon properties under physiological loads (Loren and Lieber, 1995; Loren *et al.* 1996) and used a theoretical model to predict the extent of maximum sarcomere shortening (Lieber *et al.* 1992*a*). We found that the magnitude of sarcomere shortening differed between the prime wrist movers in the order (from lowest to highest): ECRL, ECRB, extensor carpi ulnaris, flexor carpi radialis and flexor carpi ulnaris. The magnitude of sarcomere shortening for both the ECRB and ECRL was approximately $0.2 \, \mu m$ and would affect the absolute sarcomere lengths measured but not the values calculated for dSL/dω and, thus, would not affect the conclusions reached in the present study.

References

Bäckdahl, M. and Carlsöö, S. (1961). Distribution of activity in muscles acting on the wrist (an electromyographic study). *Acta. morph. neerl.-scand.* **4**, 136–144.

Brand, P. W., Beach, R. B. and Thompson, D. E. (1981). Relative tension and potential excursion of muscles in the forearm and hand. *J. Hand Surg.* **3**, 209–219.

Burkholder, T. J., Fingado, B., Baron, S. and Lieber, R. L. (1994). Relationship between muscle fiber types and sizes and muscle architectural properties in the mouse hindlimb. *J. Morph.* **220**, 1–14.

Butler, D. L., Grood, E. S., Noyes, F. R. and Zernicke, R. F. (1978). Biomechanics of ligaments and tendons. In *Exercise and Sport Sciences Review*, vol. 6, pp. 125–182. Baltimore, MD: The Franklin Institute Press.

Close, R. I. (1972). Dynamic properties of mammalian skeletal muscles. *Physiol. Rev.* **52**, 129–197.

Ebashi, S., Maruyama, K. and Endo, M. (1980). *Muscle Contraction: Its Regulatory Mechanisms*. New York: Springer Verlag.

Fridén, J. and Lieber, R. L. (1994). Physiological consequences of surgical lengthening of extensor carpi radialis brevis muscle–tendon junction for tennis elbow. *J. Hand Surg.* **19**A, 269–274.

Friederich, J. A. and Brand, R. A. (1990). Muscle fiber architecture in the human lower limb. *J. Biomech.* **23**, 91–95.

Gans, C. (1982). Fiber architecture and muscle function. In *Exercise and Sport Science Review*, vol. 10, pp. 160–207. Lexington, MA: Franklin University Press.

Gans, C. and De Vries, F. (1987). Functional bases of fiber length and angulation in muscle. *J. Morph.* **192**, 63–85.

Gordon, A. M., Huxley, A. F. and Julian, F. J. (1966). Tension development in highly stretched vertebrate muscle fibres. *J. Physiol., Lond.* **184**, 143–169.

Henneman, E., Somjen, G. and Carpenter, D. O. (1965). Functional significance of cell size in spinal motorneurons. *J. Neurophysiol.* **28**, 560–580.

Huxley, A. F. (1974). Muscular contraction. *J. Physiol., Lond.* **243**, 1–43.

Lieber, R. L. (1993). Skeletal muscle architecture: implications for muscle function and surgical tendon transfer. *J. Hand Ther.* **6**, 105–113.

Lieber, R. L. and Blevins, F. T. (1989). Skeletal muscle architecture of the rabbit hindlimb: functional implications of muscle design. *J. Morph.* **199**, 93–101.

Lieber, R. L. and Boakes, J. L. (1988). Sarcomere length and joint kinematics during torque production in the frog hindlimb. *Am. J. Physiol.* **254**, C759–C768.

Lieber, R. L. and Brown, C. G. (1993). Sarcomere length–joint angle relationships of seven frog hindlimb muscles. *Acta anat.* **145**, 289–295.

Lieber, R. L., Brown, C. G. and Trestik, C. L. (1992*a*). Model of muscle–tendon interaction during frog semitendinosus fixed-end contractions. *J. Biomech.* **25**, 421–428.

Lieber, R. L., Fazeli, B. M. and Botte, M. J. (1990). Architecture of selected wrist flexor and extensor muscles. *J. Hand Surg.* **15**, 244–250.

Lieber, R. L., Jacobson, M. D., Fazeli, B. M., Abrams, R. A. and Botte, M. J. (1992*b*). Architecture of selected muscles of the arm and forearm: anatomy and implications for tendon transfer. *J. Hand Surg.* **17**, 787–798.

Lieber, R. L., Loren, G. J. and Fridén, J. (1994). *In vivo* measurement of human wrist extensor muscle sarcomere length changes. *J. Neurophysiol.* **71**, 874–881.

Lieber, R. L., Raab, R., Kashin, S. and Edgerton, V. R. (1992*c*).

Sarcomere length changes during fish swimming. *J. exp. Biol.* **169**, 251–154.

Loren, G. J. and Lieber, R. L. (1995). Tendon biomechanical properties enhance human wrist muscle specialization. *J. Biomech.* **28**, 791–799.

Loren, G. J., Shoemaker, S. D., Burkholder, T. J., Jacobson, M. D., Fridén, J. and Lieber, R. L. (1996). Influences of human wrist motor design on joint torque. *J. Biomech.* **29**, 331–342.

Lutz, G. J. and Rome, L. C. (1994). Built for jumping: the design of the frog muscular system. *Science* **263**, 370–372.

Mai, M. T. and Lieber, R. L. (1990). A model of semitendinosus muscle sarcomere length, knee and hip joint interaction in the frog hindlimb. *J. Biomech.* **23**, 271–279.

McFarland, G. B., Krusen, U. L. and Weathersby, H. T. (1962). Kinesiology of selected muscles acting on the wrist: electromyographic study. *Arch. Phys. Med. Rehab.* **43**, 165–171.

Petit, J., Filippi, G. M., Emonet-Dénand, C., Hunt, C. C. and Laporte, Y. (1990). Changes in muscle stiffness produced by motor units of different types in peronus longus muscles of cat. *J. Neurophysiol.* **63**, 190–197.

Powell, P. L., Roy, R. R., Kanim, P., Bello, M. and Edgerton, V. R. (1984). Predictability of skeletal muscle tension from architectural determinations in guinea pig hindlimbs. *J. appl. Physiol.* **57**, 1715–1721.

Riek, S. and Bawa, P. (1992). Recruitment of motor units in human forearm extensors. *J. Neurophysiol.* **68**, 100–108.

Rome, L. C., Funke, R. P., Alexander, R. M., Lutz, G., Aldridge, H., Scott, F. and Freadman, M. (1988). Why animals have different muscle fiber types. *Nature* **335**, 824–827.

Rome, L. C. and Sosnicki, A. A. (1991). Myofilament overlap in swimming carp. II. Sarcomere length changes during swimming. *Am. J. Physiol.* **163**, 281–295.

Rome, L. C., Swank, D. and Corda, D. (1993). How fish power swimming. *Science* **261**, 340–343.

Sacks, R. D. and Roy, R. R. (1982). Architecture of the hindlimb muscles of cats: functional significance. *J. Morph.* **173**, 185–195.

Sosnicki, A. A., Loesser, K. E. and Rome, L. C. (1991). Myofilament overlap in swimming carp. I. Myofilament lengths of red and white muscle. *Am. J. Physiol.* **260**, C283–C288.

Squire, J. (1981). *The Structural Basis of Muscular Contraction.* New York: Plenum Press.

Van der Helm, F. C. T. and Veenbaas, R. (1991). Modelling the mechanical effect of muscles with large attachment sites: application to the shoulder mechanism. *J. Biomech.* **24**, 1151–1163.

Walker, S. M. and Schrodt, G. R. (1973). I-segment lengths and thin filament periods in skeletal muscle fibers of the rhesus monkey and humans. *Anat. Rec.* **178**, 63–82.

Walmsley, B., Hodgson, J. A. and Burke, R. E. (1978). Forces produced by medial gastrocnemius and soleus muscles during locomotion in freely moving cats. *J. Neurophysiol.* **41**, 1203–1216.

Walmsley, B. and Proske, U. (1981). Comparison of stiffness of soleus and medial gastrocnemius muscles in cats. *J. Neurophysiol.* **46**, 250–259.

Wickiewicz, T. L., Roy, R. R., Powell, P. L. and Edgerton, V. R. (1983). Muscle architecture of the human lower limb. *Clin. Orthop.* **179**, 275–283.

Zajac, F. E. (1992). How musculotendon architecture and joint geometry affect the capacity of muscle to move and exert force on objects: A review with application to arm and forearm tendon transfer design. *J. Hand Surg.* **17**A, 799–804.

Zuurbier, C. J. and Huijing, P. A. (1992). Influence of muscle geometry on shortening speed of fibre, aponeurosis and muscle. *J. Biomech.* **25**, 1017–1026.